Chemistry & Biology, Vol. 9, 333–344, March, 2002, ©2002 Elsevier Science Ltd. All rights reserved. PII S1074-5521(02)00115-1

Yersiniabactin Synthetase: A Four-Protein Assembly Line Producing the Nonribosomal Peptide/ Polyketide Hybrid Siderophore of *Yersinia pestis*

Deborah Ann Miller, Lusong Luo, Nathan Hillson, Thomas A. Keating, and Christopher T. Walsh[1]
Department of Biological Chemistry and
Molecular Pharmacology
Harvard Medical School
240 Longwood Avenue
Boston, Massachusetts 02115

Summary

Yersiniabactin synthetase comprises four proteins, YbtE, HMWP1, HMWP2, and YbtU, encompassing seventeen functional domains, twelve catalytic and five carrier, to select, activate, and incorporate salicylate, three cysteines, and one malonyl moiety into the iron chelator yersiniabactin (Ybt). In the present study, yersiniabactin has been reconstituted in vitro from the 4 protein assembly line by the use of eight biosynthetic precursors. The rate of one turnover, comprising 22 chemical operations performed by the assembly line to release the completed Ybt molecule, was determined at 1.4 min^{-1}. During the course of Ybt production, the elongating acyl-S-enzyme chain was shown to transfer across a nonribosomal peptide synthetase/ polyketide synthase (NRPS/PKS) interprotein interface and then a PKS/NRPS intraprotein interface. This study on the Ybt synthetase assembly line represents the first complete in vitro reconstitution of a nonribosomal peptide/polyketide hybrid system.

Introduction

When the plague bacterium *Yersinia pestis* is in iron-deficient microenvironments, this pathogenic microbe secretes the virulence factor yersiniabactin (Ybt) siderophore [1, 2] to scavenge ferric ions, e.g., from an infected vertebrate host. The four-ring structure of Ybt provides iron with six chelation donors, including the phenolic OH and the nitrogens of the thiazolidine and thiazoline rings and the terminal carboxylate. The X-ray structure for the complex of the related siderophore micacocidin A with zinc corroborated this structure [3]. The structure of Ybt suggests a hybrid origin of nonribosomal peptide and polyketide biosynthetic logic. As noted in Figure 1, labeling studies indicate that salicylate-cysteine-cysteine-malonate-cysteine are the five monomer units, assembled in that order, and that the three C-methyl groups derive from the methyl moiety of S-adenosylmethionine (SAM).

The genes for yersiniabactin production in *Y. pestis* strains are clustered in a high pathogenicity island (HPI), and DNA sequence and mutational analysis have revealed several required genes, including those for conversion of the central aromatic biosynthetic metabolite chorismate into salicylate [2, 4, 5, 6]. Most notable are two very large open reading frames, encoding *h*igh-*m*olecular-*w*eight *p*roteins 1 and 2 (HMWP1 and HMWP2). The function of three gene products contained within the HPI, YbtU, YbtT, and YbtS have yet to be validated biochemically, although they have been shown to be required in vivo [7, 8]. YbtU is about 26% similar to PchG, the NADPH-dependent reductase domain from pyochelin synthetase, the siderophore produced by *Pseudomonas aeruginosa* [9], and YbtT has a thioesterase-like domain [7]. YbtS probably catalyzes the conversion of chorismate into salicylic acid [8]. Bioinformatic analysis [8] suggested that the assembly line begins with YbtE as a salicylate-activating enzyme, followed by the 6 domain, 230 kDa HMWP2, then the 9 domain, 350 kDa HMWP1. Experimental validation of YbtE as a salicyl-AMP ligase and of HMWP2 as a 2 module NRPS that cyclized two tandem Cys-S-HMWP2 acyl enzymes to a hydroxyphenyl-thiazolinyl-thiazolinyl (HPTT)-S-enzyme has followed [8, 10, 11, 12]. HMWP1 has been shown to contain a 5 domain polyketide synthase (PKS) module followed by a 4 domain NRPS module, utilizing malonyl-CoA and cysteine, respectively [13], and to have functional C-methyltransferase activity [14]. The stage was thus set for efforts at full reconstitution of this hybrid NRPS/PKS/NRPS assembly line.

In this study we show that the combination of the four purified protein components (YbtE, HMWP2, HMWP1, and YbtU) encoded within the HPI and eight cosubstrates permit catalytic turnover of all seventeen domains to release the authentic siderophore. YbtU serves as a thiazolinyl-S-HMWP1 reductase. YbtT, the external thioesterase domain, was shown to have no effect on the rate of Ybt production; therefore, its in vivo role in Ybt biosynthesis remains obscured.

Results

Acyltransferase and Acyl Carrier Protein Domains: Substrate Specificity and Covalent Loading

Prior studies on yersiniabactin synthetase have shown the six NRPS domains of HMWP2 [11, 12, 15] and the NRPS portion of HMWP1 [14], the last four domains, to be fully functional. However, the HMWP1 PKS module, comprising the first five domains of HMWP1, has not been as extensively studied [16]. The loading of the HMWP1 acyl carrier protein (ACP) domain by its acyl transferase (AT) domain with a coenzyme A (CoA) derivative and acyl chain transfer from HMWP2 PCP_2 to this ACP are two initial functions that needed to be verified.

Only two methyltransferase (MT) domains exist within yersiniabactin synthetase, whereas three C-methylations are required to produce the final yersiniabactin structure. No clear prediction of the specificity of the AT domain of HMWP1 could be made after sequence alignment (Figure 2) and comparison to the signature motifs of AT domains previously cited [17, 18, 19, 20]. Using radiolabeled [^{14}C]-acyl-CoA derivatives in a TCA precipitation assay, we explored the AT domain speci-

[1]Correspondence: christopher_walsh@hms.harvard.edu

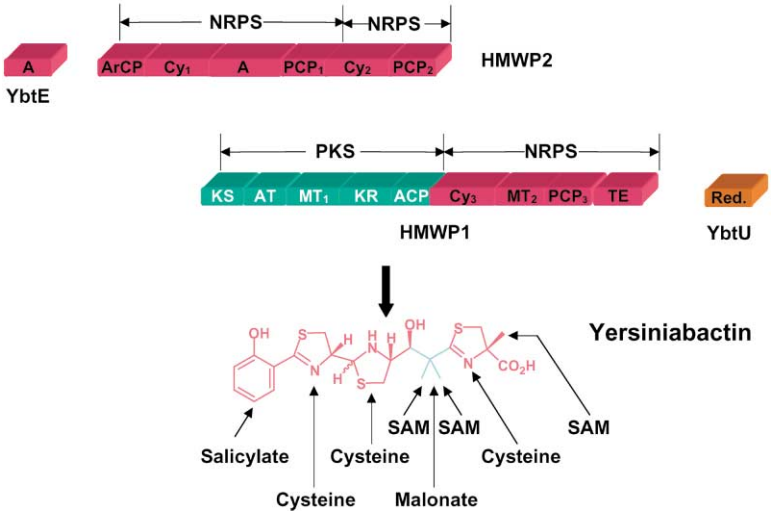

Figure 1. Yersiniabactin and the Four Proteins of Yersiniabactin Synthetase Required for In Vitro Reconstitution

YbtE is a single domain, salicyl-AMP ligase. YbtU is the putative reductase with 27% identity to PchG, the enzyme responsible for reduction during pyochelin biosynthesis in *Pseudomonas aeruginosa* [9]. HMWP2 and HMWP1 encompass the remaining 15 domains. Sterochemistry is based upon previous study of synthetic yersiniabactin (Ybt) [35]. Abbreviations are as follows: A, adenylation; ArCP, aryl carrier protein; Cy, cyclization; PCP, peptidyl carrier protein; KS, ketosynthase; AT, acyltransferase; MT, methyltransferase; KR, ketoreductase; ACP, acyl carrier protein; TE, thioesterase. The NRPS/PKS/NRPS subunits are highlighted in color. The colors of the yersiniabactin synthetase proteins correspond to the pieces they incorporate into Ybt. The eight biosynthetic precursors are shown.

ficity, and this exploration revealed the promiscuity of this HMWP1 AT. All four acyl-CoAs tested (methylmalonyl-, propionyl-, malonyl-, and acetyl-CoA) can be used as acylation substrates, although some were very slow. We then employed the rapid-quench technique to determine the kinetically preferred substrate by using KSAT, the 2 domain fragment containing the ketosynthase (KS) and acyltransferase (AT) domains of HMWP1. Single-turnover reactions of 6.5 μM KSAT enzyme with 1.5 μM [^{14}C]-malonyl-CoA or 1 μM [^{14}C]-methylmalonyl-CoA were carried out at 30°C and acid-quenched after a specified period of time (0.01–500 s). The profiles for

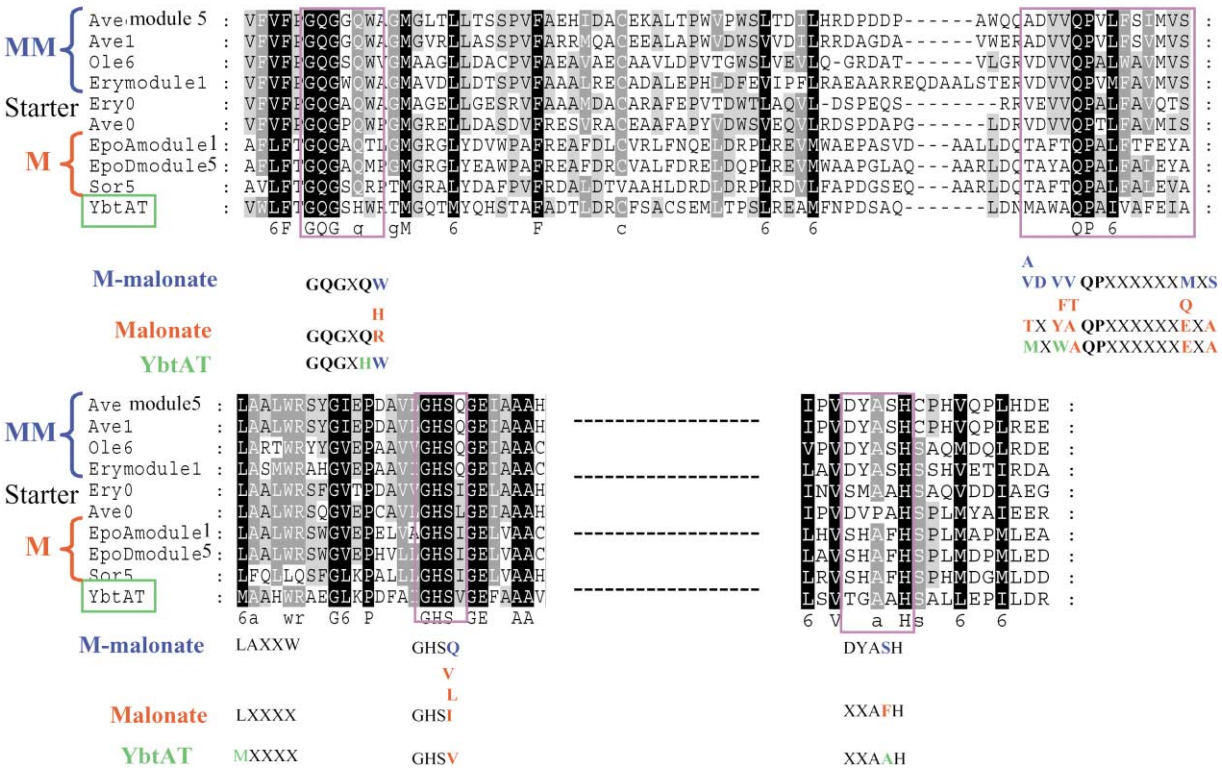

Figure 2. AT Domain Sequence Alignment

Core motifs for malonate- (red) and methylmalonate (blue)-specific AT domains [17, 18, 19, 20] are compared to that of the Ybt HMWP1 AT domain (green). Ery0 and Ave0 are two representative examples of AT domains that load starter units and have been shown to have loose AT domain specificity [36]. Ave, Ole, Ery, Epo, and Sor indicate AT domains in their corresponding modules of the moldular PKSs for avermectin, oleandomycin, erythromycin, epothiolone, and soraphen A. The sequence alignment is adapted from [17, 19]. Note that the Ybt AT domain contains conserved residues of both malonate- and methylmalonate-specific AT domains.

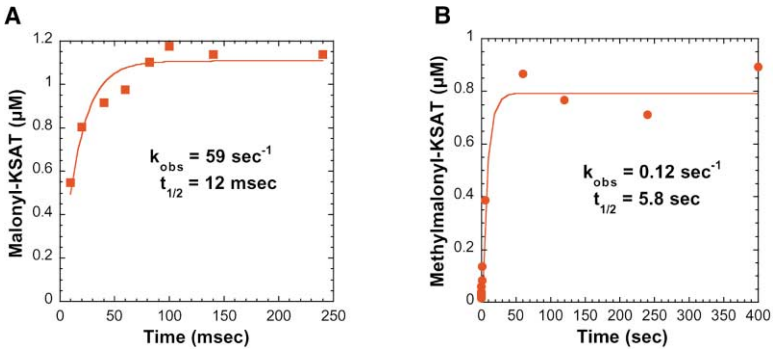

Figure 3. Time Course for the Single-Turnover Reaction Progress Curve of the Loading of the Ybt HMWP1 KSAT Fragment

Time course for the single-turnover reaction progress curve of the loading of the Ybt HMWP1 KSAT fragment with (A) malonyl-CoA and (B) methylmalonyl-CoA. Radioactivity incorporated into the KSAT fragment was measured by TCA precipitation followed by liquid scintillation counting. The curve was fitted to a first-order rate equation.

single-turnover reactions of KSAT with malonyl-CoA and methylmalonyl-CoA are shown in Figures 3A and 3B. The apparent first-order rate constant for the malonyl-CoA reaction is approximately 500-fold larger than that for the methylmalonyl-CoA reaction (59 s^{-1} versus 0.12 s^{-1}), showing that malonyl-CoA is the kinetically preferred substrate.

PCP_2, KS, and ACP Domains: Assaying the NRP/PK Switch Point

Previously we analyzed the 6 domain HMWP2 subunit, an NRPS-type assembly line that ends with the formation of the tricyclic 2-(2-hydroxyphenyl)-thiazolyl-2,4-thiazolinyl-S-enzyme (HPTT-S-enzyme) intermediate tethered in thioester linkage to its most downstream domain PCP_2 [12]. The next step in Ybt biosynthesis is in trans chain transfer to the 9 domain HMWP1 subunit. Now that malonyl-CoA was established as the kinetically preferred substrate for the AT domain, our attention turned to assaying the interprotein switch point between the NRPS module of HMWP2 and the PKS module of HMWP1. Chain transfer of HPTT-S-PCP_2 to malonyl-S-ACP would be a carbon-carbon bond-forming step as opposed to the previous two peptide bond-forming steps encoded by HMWP2.

To study the NRP/PK switch point (Figure 4A), we used a readily available simplified acyl group, acetyl, instead of the tricyclic, synthetically difficult HPTT. Sfp, a member of the phosphopantetheine transferase (PPTase) family, was used to load [^{14}C]-acetyl onto the active serine of the PCP_2 domain within S1439A, the HMWP2 mutant fragment (amino acids 1383–2035) containing an inactivated PCP_1 domain, the Cy_2 domain, and an intact PCP_2 domain. After a reaction containing the [^{14}C]-acetyl-S-PCP_2, the PKS fragment of HMWP1 (1–1896), malonyl-CoA, SAM, and NADPH, successful transfer of [^{14}C]-acetyl from HMWP2 onto the malonyl-loaded ACP was visualized by autoradiography following SDS-PAGE (Figure 4B).

MT_1 Domain: Evidence for Bis Methylation

Since we have shown that malonyl-CoA is preferred over methylmalonyl-CoA, the methyltransferase domain (MT_1), the third domain of the PKS module of HMWP1, is predicted to act twice to carry out the very unusual bis C-methylation generating the gem dimethyl group of Ybt. This hypothesis is supported by previous radioactive feeding studies, which showed that three SAM molecules are needed to produce Ybt [8]. The most likely timing of C-methylation is on a β-ketoacyl-S-ACP that

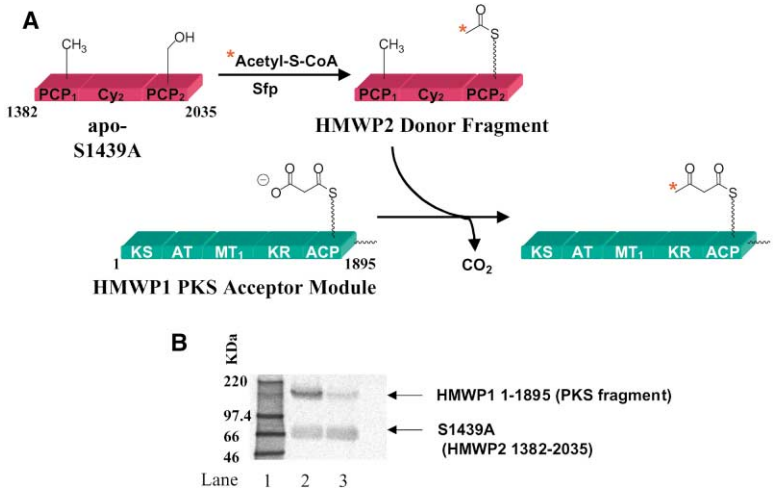

Figure 4. Assays of the Switch Point between HMWP2/HMWP1 Subunits

(A) Schematic representation of the assay used to monitor the switch point between HMWP2/HMWP1 subunits. The 3 domain apo-HMWP2 fragment S1439A contains an inactive PCP_1, Cy_2, and an intact PCP_2. The PPTase Sfp was used to posttranslationally modify the PCP_2 domain of S1439A with [^{14}C]-acetyl-CoA before addition of the malonyl-loaded PKS fragment of HMWP1. Transfer of the [^{14}C]-acetyl group from HMWP2 to the upstream nucleophilic acceptor HMWP1 was monitored via autoradiography.

(B) Autoradiogram showing that transfer of [^{14}C]-acetyl from the HMWP2 S1439A fragment to the PKS fragment (amino acids 1–1895) of HMWP1 is malonyl dependent. Lane 1, [^{14}C]-molecular-weight markers; lane 2, S1439A + PKS fragment + malonyl-CoA; lane 3, S1439A + PKS fragment without malonyl-CoA. Note that the small amount of radioactivity associated with the PKS fragment in lane 3 most likely is a result of uncatalyzed thiol exchange between the holo-ACP domain of the PKS fragment and [^{14}C]-acetyl-CoA.

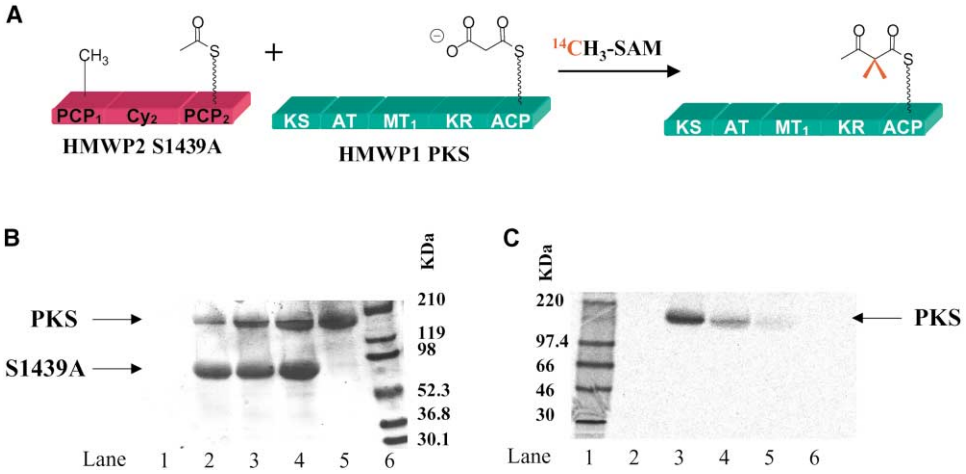

Figure 5. Assays Show that MT_1-Catalyzed Methylation Is Dependent upon the HMWP2.HMWP1 Interaction

(A) Schematic representation of the assay used to show that MT_1-catalyzed methylation is dependent upon the HMWP2/HMWP1 interaction. Sfp-modified S1439A was combined with the malonyl-loaded PKS fragment of HMWP1 in the presence of [^{14}C]-SAM. Autoradiography was used for monitoring the incorporation of radioactivity.

(B) Coomassie brilliant blue-stained 10% SDS-PAGE gel analysis.

(C) Corresponding autoradiogram. Lane 1, [^{14}C]-molecular-weight markers; lane 2, PKS + acetyl-loaded-S1439A; lane 3, PKS + acetyl-loaded-S1439A + malonyl-CoA; lane 4, PKS + apo-S1439A + malonyl-CoA; lane 5, PKS + malonyl-CoA; lane 6, molecular-weight markers.

would readily enolize and provide the low-energy carbanion required for the first and then the second methylation. This prediction was validated through the incorporation of [$^{14}CH_3$]-SAM into the PKS fragment of HMWP1 (Figure 5A) in a reaction containing acetyl-S-PCP_2, the PKS fragment of HMWP1 (1–1896), malonyl-CoA, SAM, and NADPH; this reaction was monitored by autoradiography following SDS-PAGE (Figures 5B and 5C). This methylation was shown to be dependent upon the presence of the HMWP2 fragment (lanes 4 and 5) and malonyl-CoA (lane 2). Reactions performed with unprimed or apo-S1439A (lane 4) still afforded some transfer (approximately 50% of lane 3) of radioactivity from of [$^{14}CH_3$]-SAM into the PKS fragment. This result may imply that the protein-protein interaction between the HMWP1 and HMWP2 fragments may allow one methyl group to be transferred to the malonate loaded onto the PKS fragment prior to condensation. Alternatively, this methylation may be an indication that the S1439A protein used was not completely apo, allowing slow thiol exchange between the holo-PCP_2 and malonyl-CoA, which could be transferred to the ACP and used as a substrate for methylation. We have now shown function of four (KS, AT, MT_1, and ACP) of the five domains in the PKS module of HMWP1.

Full Reconstitution of Ybt

Both switch points, the interprotein NRP/PK and the intraprotein PK/NRP, had now been assayed individually [14]. Four Ybt proteins (the stand-alone 60 KDa salicylate adenylation [A] domain YbtE, the 230 kDa NRPS HMWP2, the 350 kDa PKS/NRPS hybrid HMWP1, and the 41 kDa stand-alone reductase domain YbtU) had been overexpressed and purified as shown in Figure 6. We were now poised to assay both switch points concomitantly through full enzymatic reconstitution of Ybt. We used MALDI-TOF (matrix-assisted laser desorption ionization time-of-flight) mass spectroscopy (MS) to prove in vitro reconstitution of Ybt ([M+H]$^+$ 481.6 Da) from a reaction containing all five enzymes, salicylate, cysteine, malonyl-CoA, SAM, NADPH, and ATP (Figure 7A). We repeated the reaction in the presence of L-cysteine (3, 3-D_2) (Figure 7B) to validate the presence of three cysteines in the final product (M + 6). In addition, through the use of mass spectrometry and CD_3-SAM, we were able to show that SAM is the precursor for the three C-methylations (M + 9) and that both malonyl-CoA and methylmalonyl-CoA are able to be used for the production of Ybt (Figure 8). In addition to mass spectroscopy data, HPLC analysis showed that the product (Figure 9) of the enzymatic reaction in the presence of iron coelutes with the authentic Ybt produced in vivo.

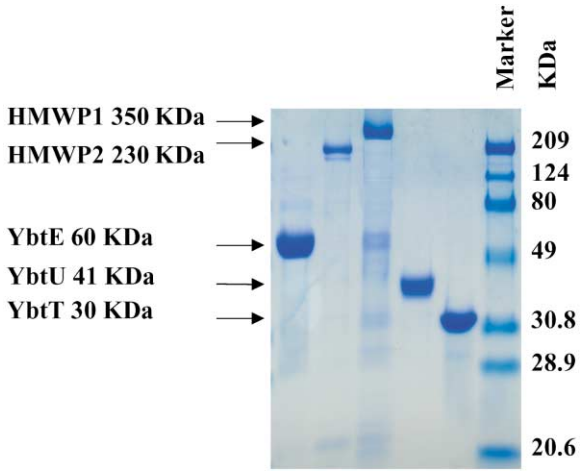

Figure 6. Coomassie Brilliant Blue-Stained 5% SDS-PAGE Gel Showing the Five Yersiniabactin Synthetase Proteins

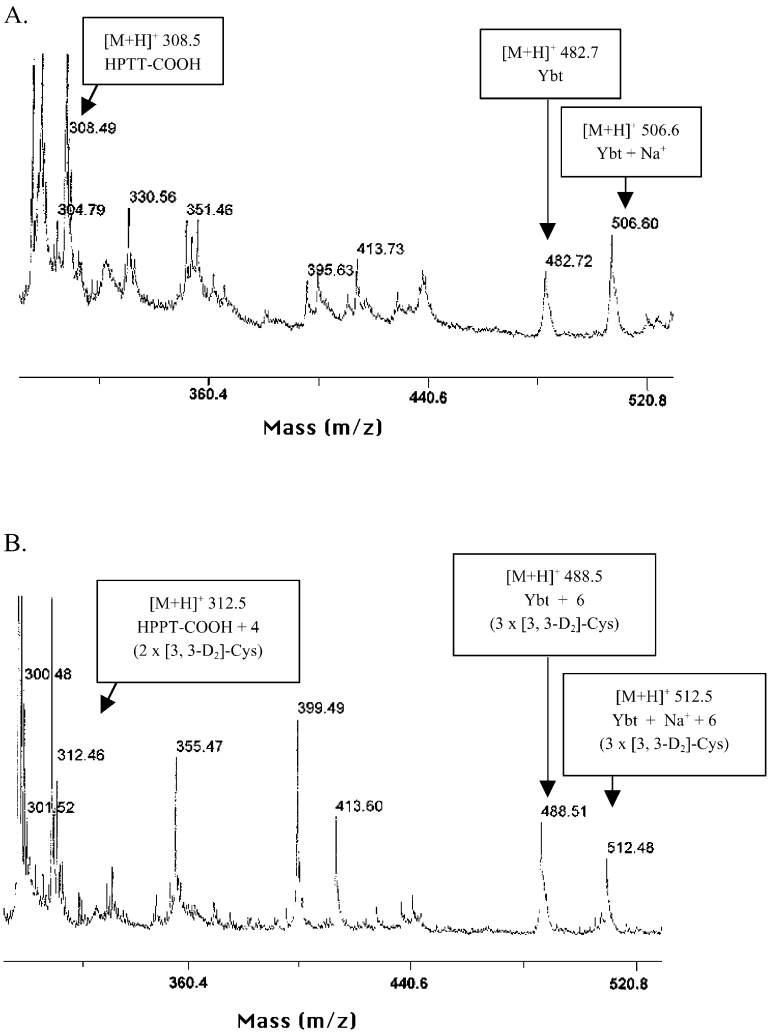

Figure 7. MALDI-TOP MS of Full Reconstitution Reaction of Ybt

The reaction was done with (A) Cysteine or (B) L-Cysteine (3,3-D_2).

Kinetics of Ybt Production

A thin-layer chromatography (TLC) assay was developed by the use of [^{14}C]-salicylate, which allows one to monitor production of both the dead-end product, HPTT-COOH, resulting from hydrolysis off of the last HMWP2 carrier protein domain PCP_2, and the complete Ybt. The data were fitted to a Michaelis-Menten equation (Figure 10), and the Km for salicylate for Ybt production was determined to be 10 μM $\pm$ 2 μM, which is comparable to the previously reported Km value of 4.6 μM for the salicylate adenylation reaction catalyzed by YbtE [10]. The four Ybt proteins (HMWP1, HMWP2, YbtE, and YbtU) catalyze the production of HPTT-COOH with a k_{cat} of 6.6 min^{-1} and that of the full Ybt with a k_{cat} of 1.4 min^{-1}, indicating that only about 20% of the enzyme bound HPTT-S-PCP_2 intermediate, produced through the action of HMWP2, is actually being transferred successfully as the electrophilic donor to HMWP1.

YbtU: The Stand-Alone Reductase Domain

The function of the reductase domain, YbtU, of reducing the second thiazoline ring to the thiazolidine was de-

CoA	SAM	$[M+H]^+_{calc}$	$[M+H]^+_{obs}$	
Malonyl- or Methylmalonyl-	CH_3-SAM	481.6	482.7	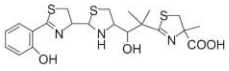
Malonyl-	CD_3-SAM	490.6	491.3	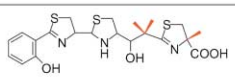
Methylmalonyl-	CD_3 -SAM	487.6	488.6	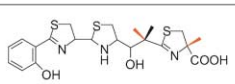

Figure 8. MS Results of Ybt Produced In Vitro with Malonyl- or Methylmalonyl-CoA and CD3-SAM as Substrates

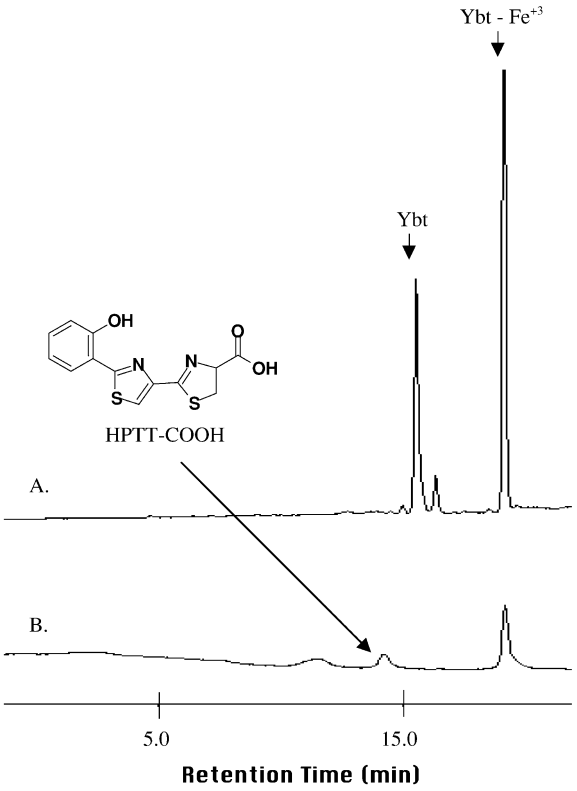

Figure 9. HPLC Traces of Authentic Ybt and Enzymatic Reconstitution Reaction Products

Labeled HPLC traces of (A) authentic Ybt and (B) reaction products from YbtE, HMWP2, HMWP1, YbtU, salicylate, cysteine, malonyl-CoA, and SAM as described in the Experimental Procedures. $FeCl_3$ was added to the reaction to enhance the UV signal. The identities of the peaks were verified by MALDI-TOF MS analysis.

duced from mass spectrometry of reactions with and without YbtU (Figure 11). In the absence of YbtU, a mass of 478.3 Da, corresponding to the $[M+H]^+$ ion of a Ybt product in which the first thiazoline ring is spontaneously oxidized to the thiazole and the thiazolidine ring remains oxidized as the thiazoline, was detected. In the presence of YbtU, the product produced had a mass of 482.7 Da, consistent with the $[M+H]^+$ ion of authentic Ybt. The oxidized HPTT-COOH ($[M+H]^+ = 308$ Da) intermediate was produced regardless of the presence of YbtU, which may indicate that the acyl chain on HMWP2 does not get reduced to thiazolidine. However, if a reduced form of HPTT-enzyme is required for transfer to HMWP1, this result may reflect the partitioning between hydrolysis and reduction of the HPTT-S-HMWP2 intermediate. Nonetheless, future studies need to be done to determine if YbtU catalyzes the reduction of the second thiazoline to thiazolidine before, during, or after the action of HMWP1.

YbtT: The External Thioesterase Domain

YbtT is a 30 KDa protein containing the G(Y/W/H)SxG signature motif and the downstream conserved GxH motif, consistent with thioesterase domains. YbtT was shown to have no effect on the in vitro rate of Ybt production as monitored through YbtT addition to the full reconstitution reaction analyzed by TLC (data not shown). Showing no effect on rate, YbtT was increased 10-fold relative to the other four proteins in the reaction and was therefore determined to be unnecessary for in vitro reconstitution of Ybt. This result is in contrast to the in vivo studies [7] that show that cells with an in-frame deletion of *ybtT* could not grow efficiently on iron-deficient medium. In a bioassay that would detect Ybt at a level of less than 6% of wild-type, Ybt was not detected in the iron-deficient supernant. Thus, YbtT was shown to have a dramatic in vivo effect but no detectable in vitro effect. The possible role of YbtT in editing mischarged carrier proteins is still being explored. A function of external TE domains in the PKS system was recently proposed by Leadlay and coworkers [21].

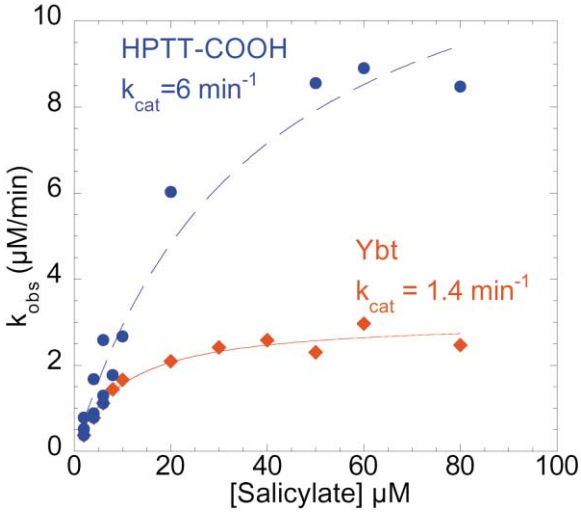

Figure 10. Michaelis-Menten Plot for the Ybt Assembly Line Reactions

The reaction was done in the presence of [^{14}C]-salicylate, spotted on a silica TLC plate, and analyzed by densitometry as described in the Experimental Procedures.

Discussion

Siderophores are elaborated by bacteria and fungi when they are starved for the essential nutrient iron. They contain any of three ferric ion chelating ligands, (1) phenols and catechols, (2) N-hydroxy groups, and (3) heterocyclic thiazolines and oxazolines (from cyclization of Cys and Ser moieties), that derive from small molecules such as salicylate, 2,3-dihydroxybenzoate (DHB), and amino acid monomers [22, 23, 24]. Thus, all siderophore synthetases examined to date are nonribosomal peptide synthetases, with the salicyl and DHB groups introduced as aryl-N-caps [25, 26].

Yersiniabactin biosynthesis is of particular interest for several reasons. First, it is a virulence factor for the causative agent of plague, and knowledge of the molecular logic of yersiniabactin synthetase may enable inhibitor design that will attenuate virulence. Second, yersiniabactin synthetase encodes many chemically interesting catalytic steps. Ybt has three five-ring sulfur- and nitro-

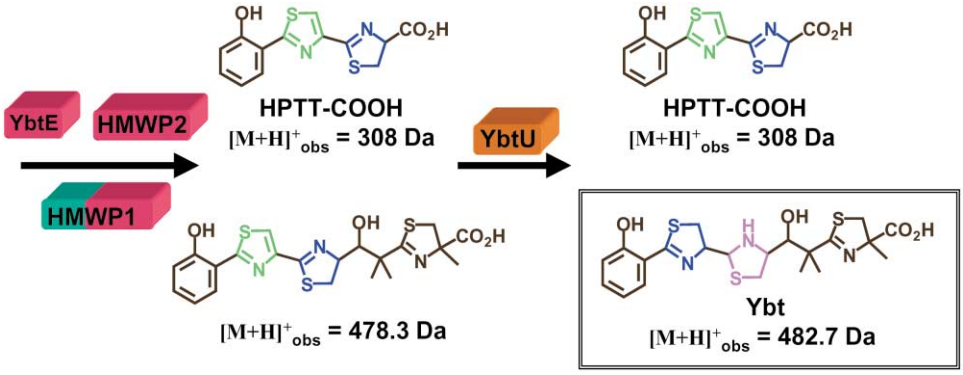

Figure 11. YbtU Catalyzes the Reduction of the Second Thiazoline Ring to Thiazolidine

As previously described [12], both enzymatic and synthetic HPTT undergo spontaneous oxidation of the first thiazoline to the heteroaromatic thiazole, adding conjugation to the second thiazoline ring. YbtU-catalyzed reduction of the second ring to the thiazolidine reduces susceptibility toward oxidation. Thiazole rings are shown in green, thiazoline in blue, and thiazolidine in pink.

gen-containing heterocycles, derived from the cyclization of cysteine during peptidyl chain elongation on the NRPS assembly line; three C-methylations, derived from three SAM cosubstrates; and a redox adjustment of one of the heterocycles (thiazoline to thiazolidine). Third, and most intriguingly, yersiniabactin is a nonribosomal peptide and polyketide hybrid, and study of this assembly line allows dissection of the merged rules of PKS and NRPS logic. A number of therapeutically important natural products, including bleomycin, rapamycin, FK506, and epothilone, are PK/NRP hybrids, and combinatorial biosynthesis efforts require understanding of the rules for how NRPS and PKS assembly lines converge.

Although we have recently reported the in vitro reconstitution of two full siderophore synthetase assembly lines, for enterobactin [27] and pyochelin [9], they have only NRPS components. The reconstitution of the Ybt synthetase assembly line reported here is the first example for a hybrid assembly line and involves two chain-switching points, from NRPS to PKS module across the interface of HMWP2 and HMWP1, then back from PKS to NRPS within the HMWP1 subunit. The HMWP2 subunit has three carrier protein domains (Figure 12). The salicyl group from salicyl-AMP is loaded on the pantetheinyl thiol of the first one (ArCP domain). On the next, PCP_1, cysteinyl-AMP is the donor for loading the Cys moiety, condensation to salicylate (Sal)-Cys follows, and then the cyclization domain (Cy_1) makes the hydroxyphenyl-thiazolinyl-S-PCP_1 (HPT-S-PCP_1). Analogously, at PCP_2 Cys is loaded covalently, the HPT donor is condensed, and then Cy_2 cyclizes to yield HPTT-S-PCP_2. Seven chemical operations have occurred, and the three-ring HPTT intermediate is docked at the most downstream of the carrier protein domains of HMWP2.

Now comes the first chain-switching point from NRPS to PKS logic, as the elongating HPTT chain is transferred in trans to the first carrier protein of the HMWP1 subunit, ACP domain, the fourth overall in the assembly line (Figure 13). The ACP domain in the PKS module that comprises the N-terminal 60% of HMWP1 must be loaded with a malonyl moiety by the AT domain of HMWP1. Chain transfer is effected by the keto synthase (KS)

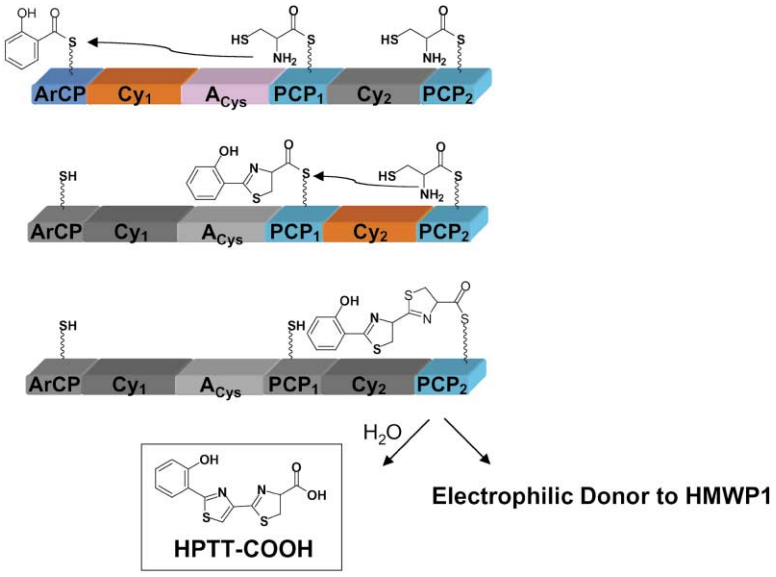

Figure 12. Seven Chemical Steps Catalyzed by HMWP2

Colored domains are responsible for the catalytic activity of that step.

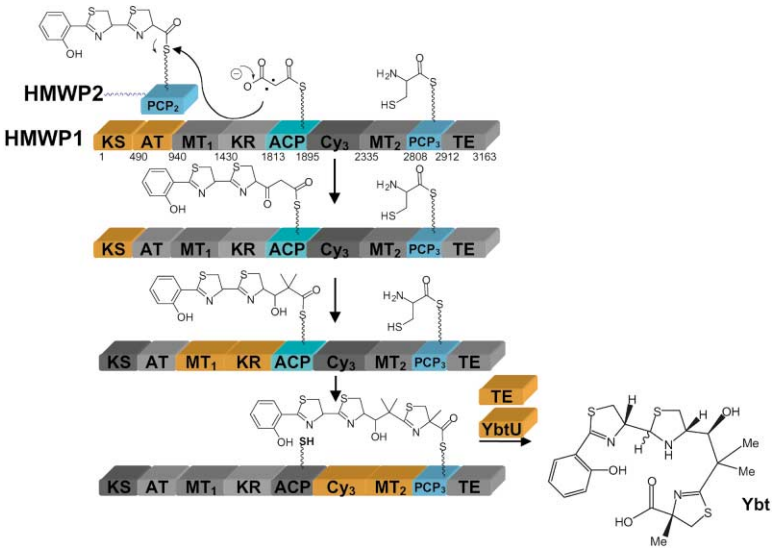

Figure 13. Fifteen Chemical Steps Catalyzed by HMWP1

Acyl intermediates are highlighted in green.

domain of HMWP1, the switch point catalyst carrying out Claisen condensation chemistry rather than the peptide bond-forming steps of NRPS condensation and cyclization domains. We will return to the other chemical steps that must occur while the chain is docked on the S-pantetheinyl-ACP way station, but note that the fifth and last carrier protein of the Ybt assembly line is PCP_3, in the NRPS module that comprises the C-terminal 40% of HMWP1. Docked on the pantetheinyl-PCP_3 is the third and last cysteinyl moiety so that chain transfer from ACP to PCP_3 constitutes the second switch point, from PKS logic back to NRPS logic. The catalyst at this switch point is Cy_3, making a peptide bond, rather than the C-C bond that occurred at the fourth way station just upstream. It will be of particular interest to probe the selectivity/promiscuity of this hybrid natural-product assembly line's two switch point catalytic domains, the KS and Cy_3 domains, to determine what combinatorial possibilities for hybrid chain elongations can be effected.

A closer examination of the chemical steps executed by the seven catalytic domains on the two carrier proteins, ACP and PCP_3, that are embedded in the 9 domain HMWP1 subunit indicate 15 chemical operations (Figure 13): at KS, acylation of its active site Cys by HPTT, decarboxylation of the malonyl-S-ACP; at AT, acylation of the active site Ser by the malonyl group; at ACP, covalent loading by malonyl, condensation to the HPTT-β-keto acyl group, C2 methylation, C2 methylation, β-keto reduction by the KR domain; at PCP_3, covalent loading with Cys, condensation by Cy_3 action; cyclization by Cy_3 action, C methylation of the Cα of the thaizolinyl-S-PCP_3 intermediate, reduction of the middle thiazoline ring by YbtU with NADPH; at the TE, acylation by the mature Ybt acyl group, and finally hydrolysis to release free Ybt-COOH into solution as the termination step of the acyl enzyme cascade. Figures 11 and 12 summarize the 22 chemical operations that go on at the five S-pantetheinyl carrier protein way stations on HMWP1 and HMWP2 of the assembly line.

Analysis of flux indicates that under the specified experimental conditions for assembly line reconstitution the twelve substrates (salicylate, three cysteines, four ATPs, NADPH, and three SAMs) undergo the 22 operations with a net throughput of 1.4 min^{-1}. Starting with [^{14}C]-salicylate radioactivity analysis for any other species found in solution in turnover amounts is a sensitive measure of whether any intermediates have fallen off from any of the carrier protein way stations. The only other species released into solution was [^{14}C]-HPTT-COOH. This accords with our earlier findings that HPTT-COOH could be released hydrolytically from the isolated HMWP2 subunit, suggesting some kinetic accessibility of water to the HPTT-S-PCP_2 acyl thioester enzyme intermediate. Also, this is the only intermediate that must undergo the in trans transfer between subunits HMWP2 to HMWP1. All other chain transfers are within either the HMWP2 or HMWP1 subunit. Thus, HPTT-S-HMWP2

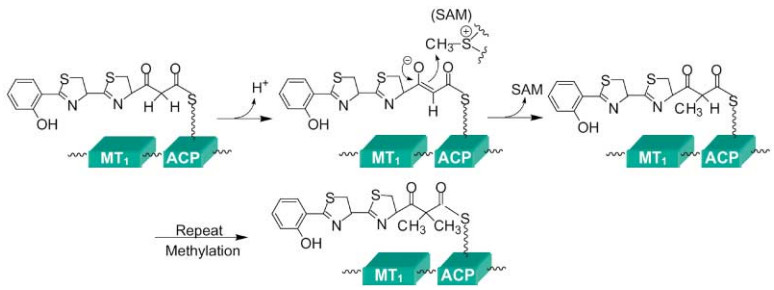

Figure 14. MT_1 Catalyzes the Transfer of the Methyl Moiety of S-Adenosyl-Methionine (SAM) and Twice Generates the Gem Dimethyl Group of Ybt

may be uniquely exposed to solvent and adventitious hydrolytic derailment. Under the current conditions, HPTT-COOH is produced at 6.6 min^{-1}, some 4.7-fold more quickly than its flux onto HMWP1 and down the line to Ybt-COOH. The successful intersubunit transfer of only 20% of the growing chains may represent suboptimal reassembly of the HMWP2 and HMWP1 subunits and will serve as an assay for improvements in catalytic efficiency of chain transfer. Previous in vivo studies have shown that intermediates fall off the assembly line at such intersubunit junctions in both the rifamycin synthase [28, 29] and the bleomycin synthetase [30, 31, 32] PKS/NRPS hybrid assembly lines. This may be an indication of weak association between the PKS/NRPS protein components in all such siderophore and antibiotic thiotemplated assembly lines.

Two chemical steps enacted by the assembly line during chain growth to mature yersiniabactin are worth note. First is the assignment of function to YbtU, known to be necessary from genetic knockout studies [7], as a thiazolinyl-S-enzyme reductase. In the absence of NADPH and YbtU, the middle thiazolinyl ring is not reduced, but the first thiazolinyl ring is autoxidized to the heteroaromatic thiazole, a net 4 electron difference from the thiazolidine of the natural product. This thiazoline reductase activity parallels our recent finding that PchG, a homolog of YbtU in the pyochelin synthetase system [9, 33], is likewise a thiazoline reductase and works only on the thiazolinyl-containing acyl chain while tethered to a peptidyl carrier protein (PCP) domain. In pyochelin, the basic thiazolidine nitrogen gets N-methylated. In micacocidin A [3] and yersiniabactin, it is likely to be a ligand to ferric iron. The second transformation is the set of C-methylations effected on the growing chain. We have recently shown that a thiazolinyl acyl group docked on PCP_3 can be methylated by the MT_2 domain of the NRPS module of HMWP1 [14]. Now, we also show that the MT_1 domain in the PKS module is a C-methyltransferase and that it acts twice since CD_3-SAM gives a Ybt product with nine deuterium atoms when malonyl-CoA is used as the substrate (Figure 8). The presumption is that the HPTT-β-ketoacyl-S-ACP intermediate can be enolized and C_3 is then a carbanion nucleophile for attack on the electropositive methyl of SAM (Figure 14). The monomethyl enolate is also chemically and kinetically competent to be methylated a second time before the acyl chain is moved downstream by the action of the Cy_3 domain. The result is a branched dimethyl tetrasubstituted carbon center that undoubtedly creates geometric constraints on the Ybt chain that will affect its conformation for iron chelation. We have also shown that the AT domain will recognize methylmalonyl-CoA in place of malonyl-CoA and this will then receive one methyl group from SAM but that flux through methylmalonyl-CoA is very low due to the gatekeeper specificity of the AT domain in favor of malonyl selection. In Figure 2, we have shown an AT domain sequence alignment. Of interest, the Ybt AT domain did not simply fit to the sequence pattern of malonyl-CoA- or methylmalonyl-CoA-specific AT regimes. A similar case was recently discovered in AT domains of another PKS/NRPS system myxalamid synthetase [19], whose specificity cannot be easily predicted by the consensus sequence proposed for malonyl-CoA or methylmalonyl-CoA.

The successful reconstitution of the 17 domain NRP/PK/NRP assembly line of yersiniabactin synthetase is a starting point for analysis of the NRP-to-PK and PK-to-NRP switch point enzyme chemistry and tolerance for what other hybrids can be built at such enzymatic interfaces. In addition, it is now possible to conduct detailed domain studies to dissect the timing of the chemical operations encoded by the KS, MT_1, and KR domains of the PKS module and those encoded by the Cy_3 and MT_2 domains of the NRPS module of the 9 domain HMWP1. It is also possible to examine how fidelity of chain modification is ensured and completed at each of the five carrier proteins before the chain is translocated to the next covalent way station downstream.

Significance

Yersiniabactin, the tetracyclic iron chelator, a virulence factor in infections by the plague bacterium *Yersinia pestis*, is a product of a hybrid assembly line of nonribosomal peptide synthetase and polyketide synthase modules. Reconstitution of the 17 domain Ybt synthetase from its four enzymatic components allows evaluation of the specificity of the catalytic domains at the NRPS/PKS interface (the KS domain) and at the PKS/NRPS interface (Cy_3) and assessment of alternate acyl chain donor and acceptor usage for combinatorial biosynthesis in such hybrid natural products. Two additional facets of the chemical transformations during chain elongation on the Ybt synthetase carrier protein domains are also of interest for mechanism and potential portability: (1) the heterocyclization of N-acyl-cysteinyl-S-PCP intermediates to thiazolinyl rings and regioselective redox adjustment to thiazolidine; and (2) the introduction of three C-methyl groups by two methyl transferase (MT) domains.

Experimental Procedures

General

ATP, Coenzyme A and derivatives, imidazole, magnesium chloride, NADPH, and S-adenosyl-L-methionine (SAM) were purchased from Sigma Chemical Co. Tris was purchased from J.T. Baker. Tris-(2-carboxyethyl)phosphine hydrochloride (TCEP) was purchased from Molecular Probes. Luria-Bertani (LB) and 2× YT Yeast Extract Tryptone media (Difco) were prepared and used for culturing *E. coli* strains. Competent cells of *E. coli* strains DH5α were purchased from GibcoBRL; cells of BL21(DE3) were purchased from Novagen. The *Pfu* DNA polymerase was bought from Stratagene. All DNA oligomers were purchased from Integrated DNA Technologies. Sfp, a phosphopantetheinyl transferase from *Bacillus subtilis*, was prepared as previously described [34]. [2-^{14}C]-malonyl-CoA (170 μM, 58.7 mCi/mmol), DL-2-[methyl-^{14}C]-malonyl-CoA (167 μM, 60 mCi/mmol), [acetyl-1-^{14}C]-CoA (388 μM, 51.6 mCi/mmol), [^{14}C]-salicylate (1.8 mM, 55.5 Ci/mol), and S-[methyl-^{14}C]-adenosyl-L-methionine ([$^{14}CH_3$]-SAM) (385 μM, 52 mCi/mmol) were purchased from New England Nuclear. HPLC analyses were performed on a Beckman System Gold equipped with a VYDAC C18 reverse-phase analytical column. Detection was at 254 nm, with mobile phase A consisting of 100 μl formic acid/200 μl triethylamine in 1 liter water and mobile phase B consisting of 4:1 acetonitrile:A. At a flow rate of 1 ml/min, a linear gradient was maintained from 10% B to 100% B over 23 min. MALDI-TOF mass spectrometry was carried out on a Perceptive Biosystems Voyager-DE STR mass spectrometer. The sequence alignment of AT domains was carried out with the program ClustalW

(European Bioinformatics Institute) and analyzed by GeneDoc (Karl Nicholas, Pittsburgh Supercomputing Center).

Overexpression and Purification of HMPW1, HMWP2, the KSAT HMWP1 Fragment, S1439A (HMWP2 1383–2035), HMWP1 (1–1896), and YbtE

HMWP1 [16], HMWP2 [12], S1439A (HMWP2 1383–2035 with a point mutation changing the active serine of PCP_1 to alanine) [11], the PKS fragment of HMWP1 (1–1896) [13], and YbtE (A_{sal} domain) [10] were prepared according to cited protocols. The KSAT HMWP1 fragment containing amino acids 1–950 was amplified by PCR from the plasmid pET28b-HMWP1 [16]. The amplicon was digested with NcoI and XhoI and ligated into the same sites of pET28b. This plasmid, pET28b-KSAT, encodes the KS domain and the AT domain fused to a C-terminal hexahistadine tag. The plasmid was transformed into *E. coli* DH5α and then into BL21 (DE3). *E. coli* BL21(DE3) cells (6L, 2× YT media, 50 μg/ml kanamycin) were grown at 30°C to an optical density (600 nm) of 0.7, cooled to 15°C, and induced with 200 μM isopropyl β-D-thiogalactopyranoside (IPTG). Cells were harvested after 7 hr, and the cell paste was resuspended in 20 mM Tris-HCl (pH 8.0) and 500 mM NaCl, lysed by French press, and purified by nickel chelate chromatography. Pure KSAT protein was dialyzed against 25 mM Tris (pH 8.0), 2 mM TCEP, and 10% glycerol, and stored at −80°C.

Overexpression and Purification of YbtU

An overexpression vector for *ybtU* was constructed from pYbtU-H6 (R. Perry, University of Kentucky) by amplification of the gene by PCR with the primer pair (forward, 5′-ATTCTTCATATGCCGTCCGC CTCCCCAAAACAAC-3′; reverse, 5′-GGATCCCTCGAGCGCCTCCT TATCATCATCGTTG-3′). The amplicon was digested with NdeI and XhoI and ligated to the same sites of pET29b. This plasmid, pET29b-YbtU, encodes *ybtU* fused to a C-terminal hexahistadine tag. The plasmid was transformed into *E. coli* DH5α and then into BL21 (DE3). The latter strain was grown (2× 1 liter) in LB media with kanamycin (40 μg/ml) for 24 hr at 22°C without IPTG induction. The cells were harvested by centrifugation, resuspended in 20 mM Tris (pH 8.0), 500 mM NaCl, and 5 mM imidazole, lysed by French press, and purified by nickel chelate chromatography. Pure YbtU was dialyzed against 25 mM Tris (pH 8.0), 100 mM NaCl, 2 mM DTT, and 10% glycerol, and stored at −80°C.

Overexpression and Purification of YbtT

The *Y. pestis ybtT* gene was amplified by polymerase chain reaction (PCR) from the plasmid pPSN345 (*irp1-ybtU-ybtT*) with the Pfu polymerase, primer 1 (5′-TGATGGCGCCTCTGTGACGCAATCTGCA ATG-3′), and primer 2 (5′-AGCGGATAACAATTTCA-3′). The PCR product was cloned into the KasI/EcoRI sites of the pPROEX-1 vector (Life Technologies) to give pYbtT-H6. The overexpression vector pYbtT-H6 (R. Perry, University of Kentucky) was transformed into *E. coli* BL21(DE3). This strain was grown (5× 1 liter) in LB media with ampicillin (100 μg/ml) at 37°C to an OD_{600} of 0.5. The temperature was then lowered to 30°C, and the cultures were induced with 400 μM IPTG. After 3 hr, the cultures were harvested at OD_{600} = 1.7. Purification of YbtT was performed according to the procedures for YbtU.

Autoradiography Demonstrating the Acyl Transfer from HMWP2 to HMWP1 and the Function of the MT_1 Domain

To demonstrate transfer across the NRPS-to-PKS switch point at the HMWP2/HMWP1 interface, we formed [^{14}C]-acetyl-S-PCP_2 on the S1439A fragment of HMWP2 by incubating Sfp (1.7 μM) with [^{14}C]-acetyl-CoA (80 μM) and apo-S1439A (74 μM) in 3 mM $MgCl_2$ for 90 min at 30°C. After removal of unbound [^{14}C]-acetyl-CoA through a Micron YM-10 spin column (Millipore), [^{14}C]-acetyl-S1439A (22 μM) in 200 mM Tris-HCl (pH 8.0), 2 mM TCEP, and 20 mM $MgCl_2$ was incubated with holo-PKS HMWP1 fragment (9 μM), 2 mM NADPH, and 2 mM SAM with and without 1.5 mM malonyl-CoA for 90 min at 30°C. Methyltransferase activity was shown through the transfer of [$^{14}CH_3$]- from [$^{14}CH_3$]-SAM into the PKS fragment of HMWP1. Sfp was used to transfer acetyl onto the PCP_2 domain of the HMWP1 apo-S1439A fragment. Reactions were incubated for 90 min at 30°C with 20 μM acetyl-loaded-S1439A fragment, apo-S1439A, or no S1439A fragment and with 200 mM Tris-HCl (pH 8.0), 20 mM $MgCl_2$, 2 mM TCEP, 1.5 mM NADPH, and 200 μM [$^{14}CH_3$]-SAM with and without 1.5 mM malonyl-CoA. Prior to being loaded onto a 4%–20% Tris-glycine gradient gel (Bio-Rad), each reaction mixture was mixed with SDS sample buffer (without reducing agent). For visualization, the gel was stained with Coomassie blue solution, destained, and soaked in Amplify (Amersham) for 15 min. The dried gel was exposed to BAS-IIIS image plates overnight and read by a Bio-Imaging Analyzer BAS1000 (Fuji).

Isolation and Identification of HPTT-COOH and Ybt Synthesized In Vitro

A solution of 5 μM HMWP2, 5 μM HMWP1, 5 μM YbtU, and 5 μM YbtE, 0.3 μM Sfp, 100 mM Tris-HCl, pH 8.0, 10 mM $MgCl_2$, 1 mM TCEP, 1 mM CoASH, 2 mM L-cysteine, 0.75 mM SAM, 0.75 mM NADPH, 2 mM malonyl-CoA, and 2 mM salicylate was incubated at 30°C for 1 hr to allow phosphopantetheinylation of the HMWP1 and HMWP2. Then, 10 mM ATP was added, and the reaction mixtures were incubated for 14 hr at 30°C. In order to increase the UV signal, we added 5 mM $FeCl_3$ to the reaction. The reactions were then centrifuged for 5 min and injected directly onto a VYDAC C18 small-pore analytical HPLC column from which the eluted peaks were collected and subjected to MALDI-TOF MS analysis. Coinjection of authentic Ybt produced in vivo and purified as previously described [6] further verified the production of Ybt.

MS Analysis of HPTT-COOH and Ybt Synthesized In Vitro

A solution (20 μl) of 1 μM HMWP2, 1 μM HMWP1, 1 μM YbtU, 1 μM YbtT, and 1 μM YbtE, 0.3 μM Sfp, 100 mM Tris-Cl (pH 8.0), 10 mM $MgCl_2$, 1 mM TCEP, 1 mM CoASH, 2 mM L-cysteine, 0.75 mM SAM, 0.75 mM NADPH, 2 mM malonyl-CoA, and 2 mM salicylate was incubated at 30°C for 1 hr to allow phosphopantetheinylation of the HMWP1 and HMWP2. Then, 10 mM ATP was added, and the reaction mixtures were incubated for 14 hr at 30°C. Prior to direct MS analysis, the reactions were desalted according to the manufacturer's instructions for the $ZipTip_{C18}$ (Millipore) pipette tips. To further confirm the identity of the synthesized products, we used L-cysteine (3,3-D_2) (Cambridge Isotope Laboratory, Massachusetts) was used as the cysteine substrate. SAM (S-methyl-D_3) (CDN Isotopes) was used for monitoring methylation in reactions containing either malonyl-CoA or methylmalonyl-CoA. The reaction products were washed through $ZipTip_{C18}$ (Millipore) pipette tips and subjected to MALDI-TOF MS analysis.

Time Course of Ybt Formation Catalyzed by HMWP1, HMWP2, YbtE, and YbtU

The reactions were carried out as described above with a slight variation. [^{14}C]-malonyl-CoA was used as a substrate. After ATP was added, the reaction mixtures (200 μl) were incubated at 37°C, and 10 μl aliquots were removed at various times, quenched with 10 μl CCl_4, and then immediately flash frozen with liquid nitrogen. One microliter of sample was applied to Silica gel TLC plates (EM Science) in order to separate the products. The TLC was developed in developing buffer containing chloroform/acetic acid/ethanol; 90:5:5 (v/v). Phosphorimages of TLC plates were obtained after 12–96 hr exposure to BAS-IIIS image plates and read by a Bio-Imaging Analyzer BAS1000 (Fuji). The image was analyzed densitometrically with Image Gauge 3.0 software. To verify the identity of in vitro production of Ybt and HPTT-COOH, we scraped each species from the silica gel TLC plate, dissolved it in acetonitrile, and then confirmed the species' identity by MALDI-TOF MS.

Michaelis-Menten Kinetics for HPTT-COOH and Ybt Production with [^{14}C]-Salicylate at 37°C

Reactions were performed as described above with varying concentrations of [^{14}C]-salicylate with 1 μM HMWP2, 1 μM HMPW1, 1 μM YbtE, and 1 μM YbtU. Each reaction mixture was 10 μl and was incubated at 37°C for 120 min, quenched with 10 μl CCl_4, and spotted on a Silica gel TLC plate and analyzed as described above.

Measurement of a Single-Turnover Time Course for Formation of the AT Domain Seryl-Acyl Intermediate

Single-turnover time courses were measured at 30°C with a rapid-quench flow apparatus from KinTek instruments. Each reaction was

initiated by mixing 15 μl of 13 μM KSAT (in 200 mM Tris-Cl [pH 7.5] and 4 mM TCEP) and 15 μl of 3 μM [^{14}C]-malonyl-CoA (58.7 mCi/mmol) or 2 μM [^{14}C]-methylmalonyl-CoA (60 mCi/mmol). After mixing, the final concentrations (total volume, 30 μl) were 6.5 μM KSAT enzyme, 100 mM Tris-HCl (pH 7.5), and 2 mM TCEP, and either 1.5 μM [^{14}C]-malonyl-CoA (58.7 mCi/mmol) or 1 μM [^{14}C]-methylmalonyl-CoA (60 mCi/mmol). After incubation for a specified period of time (0.01–5.0 s), the reaction mixture was quenched with 100 μl 10% TCA (w/v). The quenched reaction was collected in a 2 ml Eppendorf tube. After vigorous vortexing, the precipitated protein was pelleted by centrifugation for 20 min at 11600 g at 4°C. The supernatant was separated from the pellet, and the pellet was washed with 3× 800 μl of 10% TCA. The pellet was resuspended in formic acid and assayed by scintillation counting on an LS6500 Multipurpose Scintillation Counter (Beckman). The rate constants observed for the single-turnover reactions were determined by computer-fitting the data obtained from the rapid-quench experiments to the first-order rate equation by the use of the Kaleidagraph program.

$$[P]_t = [P]_{max} (1 - \exp(-kt))$$

In this equation, $[P]_t$ = product concentration at time t, $[P]_{max}$ = maximum product concentration, and k = apparent first-order rate constant.

Acknowledgments

We would like to thank Valerie Geoffroy and Robert D. Perry (University of Kentucky) for providing authentic Ybt. We are grateful to Dr. Steven Bruner for his critical reading of this manuscript. This work has been supported by the National Institutes of Health grant GM20011 to C.T.W.

Received: October 1, 2001
Revised: November 27, 2001
Accepted: November 29, 2001

References

1. Drechsel, H., Stephan, H., Lotz, R., Haag, H., Zähner, H., Hantke, K., and Jung, G. (1995). Structure elucidation of yersiniabactin, a siderophore from highly virulent yersinia strains. Liebigs. Ann. 1727–1733.
2. Bearden, S.W., Fetherston, J.D., and Perry, R.D. (1997). Genetic organization of the yersiniabactin biosynthetic region and construction of avirulent mutants in *Yersinia pestis*. Infect. Immun. *65*, 1659–1668.
3. Kobayashi, S., Nakai, H., Ikenishi, Y., Sun, W., Ozaki, M., Hayase, Y., Takeda, R., and Micacocidin, A. (1998). B and C, novel antimycoplasma agents from *Pseudomonas* sp. II. Structure elucidation. J. Antibiot. (Tokyo) *51*, 328–332.
4. Carniel, E., Guilvout, I., and Prentice, M. (1996). Characterization of a large chromosomal "high-pathogenicity island" in biotype 1B *Yersinia enterocolitica*. J. Bacteriol. *178*, 6743–6751.
5. Pelludat, C., Rakin, A., Jacobl, C.A., Schubert, S., and Heesemann, J. (1998). The Yersiniabactin biosyntheic gene cluster of *Yersinia enterocolitica*: organization and siderophore-dependent regulation. J. Bacteriol. *180*, 538–546.
6. Perry, R.D., Balbo, P.B., Jones, H.A., Fetherston, J.D., and DeMoll, E. (1999). Yersiniabactin from *Yersinia pestis*: biochemical characterization of the siderophore and its role in iron transport and regulation. Microbiology *145*, 1181–1190.
7. Geoffroy, V.A., Fetherston, J.D., and Perry, R.D. (2000). *Yersinia pestis* YbtU and YbtT are involved in synthesis of the siderophore yersiniabactin but have different effects on regulation. Infect. Immun. *68*, 4452–4461.
8. Gehring, A.M., DeMoll, E., Fetherston, J.D., Mori, I., Mayhew, G.F., Blattner, F.R., Walsh, C.T., and Perry, R.D. (1998). Iron acquisition in plague: modular logic in enzymatic biogenesis of yersiniabactin by *Yersinia pestis*. Chem. Biol. *5*, 573–586.
9. Patel, H.M., and Walsh, C.T. (2001). *In vitro* reconstitution of the *Pseudomonas aeruginosa* nonribosomal peptide synthesis of pyochelin: characterization of backbone tailoring thiazoline reductase and N-methyltransferase activities. Biochemistry *40*, 9023–9031.
10. Gehring, A.M., Mori, I., Perry, R.D., and Walsh, C.T. (1998). The nonribosomal peptide synthetase HMWP2 forms a thiazoline ring during biogenesis of yersiniabactin, an iron-chelating virulence factor of *Yersinia pestis*. Biochemistry *37*, 11637–11650.
11. Suo, Z., Walsh, C.T., and Miller, D.A. (1999). Tandem heterocyclization activity of the multidomain 230 kDa HMWP2 subunit of *Yersinia pestis* yersiniabactin synthetase: interaction of the 1–1382 and 1383–2035 fragments. Biochemistry *38*, 14023–14035.
12. Keating, T.A., Miller, D.A., and Walsh, C.T. (2000). Expression, purification, and characterization of HMWP2, a 229 kDa, six domain protein subunit of Yersiniabactin synthetase. Biochemistry *39*, 4729–4739.
13. Suo, Z., Tseng, C.C., and Walsh, C.T. (2001). Purification, priming, and catalytic acylation of carrier protein domains in the polyketide synthase and nonribosomal peptidyl synthetase modules of the HMWP1 subunit of yersiniabactin synthetase. Proc. Natl. Acad. Sci. USA *98*, 99–104.
14. Miller, D.A., Walsh, C.T., and Luo, L. (2001). C-methyltransferase and cyclization domain activity at the intraprotein PK/NRP switch point of yersiniabactin synthetase. J. Am. Chem. Soc. *123*, 8434–8435.
15. Miller, D.A., and Walsh, C.T. (2001). Yersiniabactin synthetase: probing the recognition of carrier protein domains by the catalytic heterocyclization domains, Cy1 and Cy2, in the chain-initiating HMWP2 subunit. Biochemistry *40*, 5313–5321.
16. Suo, Z., Chen, H., and Walsh, C.T. (2000). Acyl-CoA hydrolysis by the high molecular weight protein 1 subunit of yersiniabactin synthetase: mutational evidence for a cascade of four acyl-enzyme intermediates during hydrolytic editing. Proc. Natl. Acad. Sci. USA *97*, 14188–14193.
17. Haydock, S.F., Aparicio, J.F., Molnar, I., Schwecke, T., Khaw, L.E., Konig, A., Marsden, A.F., Galloway, I.S., Staunton, J., and Leadlay, P.F. (1995). Divergent sequence motifs correlated with the substrate specificity of (methyl)malonyl-CoA:acyl carrier protein transacylase domains in modular polyketide synthases. FEBS Lett. *374*, 246–248.
18. Katz, L. (1997). Manipulation of modular polyketide synthases. Chem. Rev. *97*, 2557–2575.
19. Silakowski, B., Nordsiek, G., Kunze, B., Blocker, H., and Muller, R. (2001). Novel features in a combined polyketide synthase/non-ribosomal peptide synthetase: the myxalamid biosynthetic gene cluster of the myxobacterium *Stigmatella aurantiaca* Sga15. Chem. Biol. *8*, 59–69.
20. Ikeda, H., Nonomiya, T., Usami, M., Ohta, T., and Omura, S. (1999). Organization of the biosynthetic gene cluster for the polyketide anthelmintic macrolide avermectin in *Streptomyces avermitilis*. Proc. Natl. Acad. Sci. USA *96*, 9509–9514.
21. Heathcote, M.L., Staunton, J., and Leadlay, P.F. (2001). Role of type II thioesterases: evidence for removal of short acyl chains produced by aberrant decarboxylation of chain extender units. Chem. Biol. *8*, 207–220.
22. Neilands, J.B. (1995). Siderophores: structure and function of microbial iron transport compounds. J. Biol. Chem. *270*, 26723–26726.
23. Telford, J.R., and Raymond, K.N. (1996). Comprehensive Supramolecular Chemistry. (Pxfprd, UK: Elsevier Science).
24. Braun, V., and Hantke, K. (1997) Transition metals in microbial metabolism. (Amsterdam: Harwood).
25. Konz, D., and Marahiel, M.A. (1999). How do peptide synthetases generate structural diversity? Chem. Biol. *6*, R39–48.
26. Drechsel, H., and Jung, G. (1998). Peptide siderophores. J. Pept. Sci. *4*, 147–181.
27. Gehring, A.M., Mori, I., and Walsh, C.T. (1998). Reconstitution and characterization of the *Escherichia coli* enterobactin synthetase from EntB, EntE, and EntF. Biochemistry *37*, 2648–2659.
28. Yu, T.W., Shen, Y., Doi-Katayama, Y., Tang, L., Park, C., Moore, B.S., Hutchinson, C.R., and Floss, H.G. (1999). Direct evidence that the rifamycin polyketide synthase assembles polyketide chains processively. Proc. Natl. Acad. Sci. USA *96*, 9051–9056.
29. Stratmann, A., Toupet, C., Schilling, W., Traber, R., Oberer, L., and Schupp, T. (1999). Intermediates of rifamycin polyketide

synthase produced by an *Amycolatopsis mediterranei* mutant with inactivated rifF gene. Microbiology *145*, 3365–3375.
30. Takita, T. (1984). The bleomycins: properties, biosynthesis, and fermentation. Drugs Pharm. Sci. *22*, 595–603.
31. Takita, T., and Muroka, Y. (1990). Biosynthesis and chemical synthesis of bleomycin. In Biochemistry of Peptide Antibiotics: Recent Advances in the Biotechnology of L–Lactams and Microbial Peptides. (New York: W. de Gruyter).
32. Shen, B., Du, L., Sanchez, C., Chen, M., and Edwards, D.J. (1999). Bleomycin biosynthesis in *Streptomyces verticillus* ATCC15003: a model of hybrid peptide and polyketide biosynthesis. Bioorg. Chem. *27*, 155–171.
33. Reimmann, C., Patel, H.M., Serino, L., Barone, M., Walsh, C.T., and Haas, D. (2001). Essential PchG-dependent reduction in pyochelin biosynthesis *of Pseudomonas aeruginosa*. J. Bacteriol. *183*, 813–820.
34. Quadri, L.E., Weinreb, P.H., Lei, M., Nakano, M.M., Zuber, P., and Walsh, C.T. (1998). Characterization of Sfp, a *Bacillus subtilis* phosphopantetheinyl transferase for peptidyl carrier protein domains in peptide synthetases. Biochemistry *37*, 1585–1595.
35. Ino, A., and Murabayashi, A. (2000). Synthetic studies of thiazoline and thiazolidine-containing natural products. Part 3: total synthesis and absolute configuration of the siderophore yersiniabactin. Tetrahedron *57*, 1897–1902.
36. Lau, J., Cane, D.E., and Khosla, C. (2000). Substrate specificity of the loading didomain of the erythromycin polyketide synthase. Biochemistry *39*, 10514–10520.